BRAIN
ORIGINAL ARTICLE

The clinical and molecular spectrum of *ZFYVE26*-associated hereditary spastic paraplegia: SPG15

Afshin Saffari,[1,2] Melanie Kellner,[3,4] Catherine Jordan,[1] Helena Rosengarten,[1] Alisa Mo,[1] Bo Zhang,[1,5] Oleksandr Strelko,[1,6] Sonja Neuser,[7] Marie Y. Davis,[8,9] Nobuaki Yoshikura,[10] Naonobu Futamura,[11] Tomoya Takeuchi,[12] Shin Nabatame,[13] Hiroyuki Ishiura,[14] Shoji Tsuji,[15,16] Huda Shujaa Aldeen,[17] Elisa Cali,[17] Clarissa Rocca,[17] Henry Houlden,[17] Stephanie Efthymiou,[17] Birgit Assmann,[2] Grace Yoon,[18] Bianca A. Trombetta,[19] Pia Kivisäkk,[19] Florian Eichler,[20] Haitian Nan,[21] Yoshihisa Takiyama,[21,22] Alessandra Tessa,[23] Filippo M. Santorelli,[23] Mustafa Sahin,[1,6] Craig Blackstone,[24] Edward Yang,[25] Rebecca Schüle[3,4] and Darius Ebrahimi-Fakhari[1,26,27,28]

In the field of hereditary spastic paraplegia (HSP), progress in molecular diagnostics needs to be translated into robust phenotyping studies to understand genetic and phenotypic heterogeneity and to support interventional trials. *ZFYVE26*-associated hereditary spastic paraplegia (HSP-*ZFYVE26*, SPG15) is a rare, early-onset complex HSP, characterized by progressive spasticity and a variety of other neurological symptoms. While prior reports, often in populations with high rates of consanguinity, have established a general phenotype, there is a lack of systematic investigations and a limited understanding of age-dependent manifestation of symptoms. Here we delineate the clinical, neuroimaging and molecular features of 44 individuals from 36 families, the largest cohort assembled to date. Median age at last follow-up was 23.8 years covering a wide age range (11–61 years). While symptom onset often occurred in early childhood [median: 24 months, interquartile range (IQR) = 24], a molecular diagnosis was reached at a median age of 18.8 years (IQR = 8), indicating significant diagnostic delay. We demonstrate that most patients present with motor and/or speech delay or learning disabilities. Importantly, these developmental symptoms preceded the onset of motor symptoms by several years. Progressive spasticity in the lower extremities, the hallmark feature of HSP-*ZFYVE26*, typically presents in adolescence and involves the distal lower limbs before progressing proximally. Spasticity in the upper extremities was seen in 64%. We found a high prevalence of extrapyramidal movement disorders including cerebellar ataxia (64%) and dystonia (11%). Parkinsonism (16%) was present in a subset and showed no sustained response to levodopa. Cognitive decline and neurogenic bladder dysfunction progressed over time in most patients. A systematic analysis of brain MRI features revealed a common diagnostic signature consisting of thinning of the anterior corpus callosum, signal changes of the anterior forceps and non-specific cortical and cerebellar atrophy. The molecular spectrum included 45 distinct variants, distributed across the protein structure without mutational hotspots. Spastic Paraplegia Rating Scale scores, SPATAX Disability Scores and the Four Stage Functional Mobility Score showed moderate strength in representing the proportion of variation between disease duration and motor dysfunction. Plasma neurofilament light chain levels were significantly elevated in all patients (Mann–Whitney U-test, $P < 0.0001$) and were correlated inversely with age (Spearman's rank correlation coefficient $r = -0.65$, $P = 0.01$). In summary, our systematic cross-sectional analysis of HSP-*ZFYVE26* patients across a wide age-range, delineates core clinical, neuroimaging and molecular features and identifies markers of disease severity. These results raise awareness to this rare disease, facilitate an early diagnosis and create clinical trial readiness.

Received June 23, 2022. Revised September 14, 2022. Accepted October 02, 2022. Advance access publication October 31, 2022

1 Department of Neurology, Boston Children's Hospital, Harvard Medical School, Boston, MA, USA
2 Division of Child Neurology and Inherited Metabolic Diseases, Heidelberg University Hospital, Heidelberg, Germany
3 Department of Neurodegenerative Diseases, Hertie Institute for Clinical Brain Research and Center of Neurology, University of Tübingen, Tübingen, Germany
4 German Center for Neurodegenerative Diseases (DZNE), Tübingen, Germany
5 ICCTR Biostatistics and Research Design Center, Boston Children's Hospital, Harvard Medical School, Boston, MA, USA
6 Rosamund Stone Zander Translational Neuroscience Center, Boston Children's Hospital, Harvard Medical School, Boston, MA, USA
7 Institute of Human Genetics, University of Leipzig Medical Center, Leipzig, Germany
8 Department of Neurology, University of Washington, Seattle, WA, USA
9 Department of Neurology, VA Puget Sound Healthcare System, Seattle, WA, USA
10 Department of Neurology, Gifu University Graduate School of Medicine, Gifu, Japan
11 Department of Neurology, National Hospital Organization Hyogo-Chuo National Hospital, Ohara, Sanda, Japan
12 Department of Neurology, Japanese Red Cross Aichi Medical Center Nagoya Daiichi Hospital, Aichi, Japan
13 Department of Pediatrics, Osaka University Graduate School of Medicine, Suita, Osaka, Japan
14 Department of Neurology, Graduate School of Medicine, The University of Tokyo, Tokyo, Japan
15 Department of Molecular Neurology, Graduate School of Medicine, The University of Tokyo, Tokyo, Japan
16 Institute of Medical Genomics, International University of Health and Welfare, Chiba, Japan
17 Department of Neuromuscular Disorders, UCL Queen Square Institute of Neurology, University College London, London, UK
18 Divisions of Clinical and Metabolic Genetics and Neurology, Department of Paediatrics, The Hospital for Sick Children, University of Toronto, Toronto, Canada
19 Alzheimer's Clinical and Translational Research Unit, Department of Neurology, Massachusetts General Hospital, Boston, MA, USA
20 Department of Neurology, Massachusetts General Hospital, Harvard Medical School, Boston, MA, USA
21 Department of Neurology, Graduate School of Medical Sciences, University of Yamanashi, Yamanashi, Japan
22 Department of Neurology, Fuefuki Central Hospital, Yamanashi, Japan
23 Department of Molecular Medicine, IRCCS Fondazione Stella Maris, 56128 Pisa, Italy
24 Movement Disorders Division, Department of Neurology, Massachusetts General Hospital, Harvard Medical School, Boston, MA, USA
25 Division of Neuroradiology, Department of Radiology, Boston Children's Hospital, Harvard Medical School, Boston, MA, USA
26 Movement Disorders Program, Department of Neurology, Boston Children's Hospital, Harvard Medical School, Boston, MA, USA
27 The Manton Center for Orphan Disease Research, Boston Children's Hospital, Boston, MA, USA
28 Intellectual and Developmental Disabilities Research Center, Boston Children's Hospital, Boston, MA, USA

Correspondence to: Darius Ebrahimi-Fakhari, MD, PhD
Department of Neurology, Boston Children's Hospital
300 Longwood Avenue, Boston, MA, 02215, USA
E-mail: darius.ebrahimi-fakhari@childrens.harvard.edu

Keywords: hereditary spastic paraplegia; movement disorders; ataxia; speech delay; thin corpus callosum

Introduction

Autosomal recessive forms of hereditary spastic paraplegia (HSP) are a large, heterogenous group of rare, progressive disorders,[1] often first presenting with non-specific symptoms during childhood.[2] Molecular testing is typically not pursued until progressive spasticity becomes evident. In recent years, the increasing availability of next-generation sequencing has enabled a diagnosis in many patients with previously undefined forms of spastic paraplegia. This progress in gene discovery and molecular diagnostics now needs to be translated into robust phenotyping studies that provide a foundation for future interventional trials. Detailed cross-sectional analyses, followed by longitudinal natural history studies, provide the necessary framework for understanding genetic heterogeneity and phenotypic pleiotropy and hold the potential to galvanize international collaboration and partnerships between patients, patient advocates, physicians and researchers. This is of particular importance given the rare nature of many autosomal recessive HSPs and the urgent need for natural history data to support the development of novel molecular therapies.

ZFYVE26-associated hereditary spastic paraplegia (HSP-*ZFYVE26* or SPG15)[3] is a rare form of early-onset complex hereditary spastic paraplegia, characterized by progressive spasticity that begins in the lower extremities and is associated with several symptoms resulting from central and peripheral nervous system

dysfunction.[4] While prior reports of small case series, often in populations with high rates of consanguinity, have established a general phenotype,[5–19] a timely clinical diagnosis, counselling of families and development of research protocols is limited by the lack of systematic investigations of the clinical and molecular spectrum including an assessment of the age-dependent manifestation of symptoms.

Here, we report a detailed cross-sectional analysis of clinical, radiographic, and molecular features of 44 patients from 36 families with HSP-*ZFYVE26*. We compare our findings to previously reported cases, affirm a core set of clinical and imaging features, describe early disease manifestations and progression in a standardized manner and provide general recommendations for management and surveillance.

Subjects and methods

Clinical characterization

This study was approved by Institutional Review Boards at participating centre (Boston Children's Hospital IRB-A00033016-6, University of Tübingen IRB 423/2019BO1, IRCCS Fondazione Stella Maris IRB-HSP-PBP-102/20, University of Yamanashi #734 & #953). Patients with bi-allelic variants in *ZFYVE26* were recruited from the International Registry for Early-Onset Hereditary Spastic Paraplegia (NCT04712812), the Treat-HSP network (NCT03981276) and the JASPAC Consortium.[20] Only patients with variants classified as pathogenic or likely pathogenic according to the latest ACMG criteria[21] were included. A cross-sectional analysis of demographic, clinical and molecular data was conducted using a standardized questionnaire.[22] Rating scales including the Spastic Paraplegia Rating Scale (SPRS)[23] ($n = 28$), the SPRS Spasticity Subscore ($n = 34$),[22] Four Stage Functional Mobility Score (1 = unlimited walking; 2 = walking without aid but unable to run; 3 = walking with aid; and 4 = wheelchair-dependent, $n = 43$) and the SPATAX Disability Score[24] ($n = 28$) were applied. Brain MRI scans from 33 patients were scored and brain MRI scans from 15 patients were available for a detailed quantitative and qualitative analysis. Previously reported cases were ascertained through a systematic literature research, yielding 65 patients from 26 references which are summarized in Supplementary Fig. 1 and Supplementary Table 1. For Supplementary Table 2, phenotypic information was translated into standardized Human Phenotype Ontology (HPO) terms (v1.7.15).[25]

Molecular characterization

Bi-allelic variants in *ZFYVE26* were identified in all 44 patients (molecular diagnoses were made between January 2008 and November 2021), most commonly identified by exome sequencing ($n = 22$), multi-gene panels ($n = 12$), single gene testing ($n = 9$) or chromosomal microarray ($n = 1$). All variants were harmonized to the canonical Ensembl transcript ENST00000347230.9 (RefSeq NM_015346.4) of the GRCh38/hg38 human reference genome build using the Mutalyzer Nomenclature Checker web tool[26] and VarSome.[27] Variants were classified according to American College of Medical Genetics and Genomics (ACMG) criteria[21] using InterVar[28] and Varsome[27] (Supplementary Table 3).

Modelling of ZFYVE26 protein structure and reported variants

Protein sequence and functional annotation of human ZFYVE26 were obtained from the Universal Protein Resource (UniProt) database (UniProt ID: Q68DK2)[29] and recent publications.[30] New exonic variants identified in this study, as well as previously reported pathogenic variants, were annotated along the protein structure. CADD PHRED scores (version 1.6)[31] of all possible nucleotide substitutions of the *ZFYVE26* transcript were computed and mapped to the corresponding linear protein model using VarMAP.[32,33]

Quantification of neurofilament light chain levels

Plasma samples were obtained by standard venipuncture and collected in lithium-heparin coated BD Vacutainer PST tubes (BD #367962) for probands or EDTA-containing tubes (BD #366643) in matched controls (Supplementary Table 4). Samples were centrifuged at 2000×*g* within 30 minutes, aliquoted in cryovials and stored at −80°C. The pre-analytical interval was ≤3 days for all samples, well within the window of stability for neurofilament light chain (NfL)[34] (Supplementary Table 4). NfL plasma concentrations were measured using the HD-X NfL kit (Quanterix #103186) on the SiMoA HD-X Analyzer (Quanterix). Plasma samples were centrifuged at 10 000*g* for 5 min and diluted 1:4 in sample buffer. All samples were run in duplicates according to the manufacturer's protocol. Data were normalized across multiple batches using two kit-provided controls and two pooled plasma controls to adjust for inter-batch variability. The assay has a lower limit of quantification of 0.174 pg/ml, a limit of detection of 0.038 pg/ml (range 0.003–0.079 pg/ml) and a dynamic range in plasma of 0–1800 pg/ml.

Statistical analysis

Statistical analysis was performed using R version 4.2.0 (2022–04–22) and RStudio (version 2022.02.2 + 485; RStudio, Inc.). Demographic data were summarized using frequency counts and percentages of the total study population for categorical variables and with either mean and standard deviation (SD) or median and interquartile range (IQR) for continuous variables, depending on the distribution of data tested by visualization with histograms, quantile-quantile plots and normality testing using the Shapiro–Wilk test. Sample sizes are indicated (n) for each analysis. Linear regression analysis and, in case of repeated measures collected for some individuals, linear mixed-effects regression analysis was conducted to quantify the extent to which a dependent variable can be predicted from an independent variable. For linear regression models, the adjusted coefficient of determination (R^2_{adj}) was reported. For linear mixed-effects regression models that take into account several variance components, including fixed and random effects, both the marginal coefficient of determination (R^2_m, variance explained by fixed effects only) and the conditional coefficient of determination (R^2_c, variance explained by both fixed and random effects) were reported, as defined by Nakagawa and Schielzeth.[35,36] To determine correlations between quantitative imaging metrics, disease scores, or neurofilament light chain levels, Spearman's rank correlation coefficient (r) was calculated. Mann–Whitney U-test was performed to test the difference in plasma neurofilament light chain levels.

Data availability

The authors confirm that the data supporting the findings of this study are available upon reasonable request.

Results

Demographic and anthropometric features

This study included 44 patients from 36 families with HSP-*ZFYVE26* (Table 1 and Supplementary Table 2). Forty-one patients were reported for the first time and new, or follow up data, were reported for three cases.[6,37] Demographic information of this cohort and previously reported patients is summarized in Table 1. The ratio of male-to-female patients was 3.4:1. The median age at last follow up was 23.8 years (range: 11–61 years). Most individuals were of European or Asian background, likely reflecting the locations of the participating centres. Anthropometric data at last follow-up showed a median height and weight corresponding to −0.6 SD (IQR = 0.7) and 1.4 SD (IQR = 1.5) according to sex- and age-appropriate CDC growth charts. No characteristic facial features were noted.

Table 1 Synopsis of demographic, clinical and neuroimaging findings in HSP-*ZFYVE26* (SPG15) in the present cohort and in previously reported patients

	This cohort ($n = 44$)[a]	Previously reported cases ($n = 65$)
Demographic data		
Sex (male: female)	34:10 (77%:23%); $n = 44$	26:30 (46%:54%); $n = 56$
Ethnicity/Origin	European: 66% (29/44)	European: 36% (17/48)
	Middle Eastern: 14% (6/44, 4 Turkish, 2 Arab)	Middle Eastern: 19% (9/44, 4 Turkish, 4 Arab, 1 Iranian)
	East Asian: 11% (5/44)	East Asian: 10% (5/48)
	North African: 5% (2/44)	North African: 29% (14/48)
	Indian subcontinent: 2% (1/44)	Indian subcontinent: 4% (2/48)
	Hispanic 2% (1/44)	Hispanic: 2% (1/48)
Consanguinity	34% (12/35, NA = 1)	35% (23/65)
Development and cognitive symptoms		
Developmental delay	68% (25/37, NA = 7)	11% (7/65)
Delayed speech development	64% (23/36, NA = 8)	3% (2/65)
Delayed motor development	21% (7/33, NA = 11)	2% (1/65)
Cognitive impairment	89% (34/38, NA = 6)	62% (40/65)
Progressive cognitive decline	69% (25/35, NA = 9)	23% (15/65)
Motor symptoms		
Spasticity	Lower limbs: 98% (43/44)	Lower limbs: 65% (42/65)
	Upper limbs: 64% (28/44)	Upper limbs: 22% (14/65)
Muscle wasting	Lower limbs: 23% (10/44)	Lower limbs: 31% (20/65)
	Upper limbs: 16% (7/44)	Upper limbs: 9% (6/65)
Pyramidal signs	98% (43/44)	82% (53/65)
Contractures	30% (11/37, NA = 7)	2% (1/65)
Ataxia	64% (28/44)	8% (5/65)
Dysarthria	68% (30/44)	42% (27/65)
Nystagmus	27% (12/44)	18% (12/65)
Dystonia	11% (5/44)	5% (3/65)
Postural tremor	18% (8/44)	11% (7/65)
Parkinsonism	16% (7/44)	8% (5/65)
Level of ambulation	I: 9% (4/43, NA = 1)	I: 6% (3/48)
	II: 30% (13/43, NA = 1)	II: 13% (6/48)
	III: 28% (12/43, NA = 1)	III: 33% (16/48)
	IV: 33% (14/43, NA = 1)	IV: 48% (23/48)
Musculoskeletal symptoms		
Foot deformity	28% (11/39, NA = 5)	22% (14/65)
Scoliosis	21% (7/34, NA = 10)	9% (6/65)
Peripheral and autonomic symptoms		
Peripheral polyneuropathy	38% (10/26, NA = 18)	46% (30/65)
Urinary urgency/incontinence	54% (22/41, NA = 3)	26% (17/65)
Ocular and auditory symptoms		
Retinopathy	11% (4/35, NA = 9)	18% (12/65)
Hearing impairment	0% (0/37, NA = 7)	2% (1/65)
Brain MRI findings		
Thin corpus callosum	100% (33/33)	54% (35/65)
'Ears of the lynx' sign	76% (16/21, NA = 12)	12% (8/65)
Periventricular white matter abnormalities	94% (30/32, NA = 1)	42% (27/65)
Cerebral atrophy	34% (11/32, NA = 1)	23% (15/65)
Cerebellar atrophy	34% (11/32, NA = 1)	NA
Rating scale		
SPRS score	25.2 ± 13.3 (range 4–48, $n = 28$)	22.5 ± 9.7 (range 8–28, $n = 4$)

[a]Three previously reported patients[6,37] were counted towards the present cohort given the availability of additional and follow-up data.
NA = not available.

First clinical symptoms

There was no evidence for an increased prevalence of pre-, peri- or neonatal complications. Birth weight was normal in all individuals. Median age at first reported symptom was 24 months (IQR = 24), while the age at molecular diagnosis of HSP-*ZFYVE26* was 18.8 years (IQR = 8), corresponding to a median diagnostic delay of 14.4 years (IQR = 4.6) for those with sufficient information available. The first reported symptom was mild developmental delay in 25/37 cases, most commonly mild speech delay (23/36) (Table 1). Gross motor milestones were usually achieved within expected time frames: Unsupported sitting was attained at a median age of 6 months (IQR = 2), while unsupported walking was met at a median of 14 months (IQR = 6). Six individuals never achieved independent walking and were always dependent on assistance or walking aids. Anecdotally, a history of mild learning disability was common in this cohort. There were no reports of developmental regression in early childhood.

Spasticity and motor symptoms

The first reported motor symptom in early childhood consisted of 'balance problems' and 'clumsiness' in most cases. Spasticity in the lower extremities was eventually present in nearly all patients (Table 1 and Videos 1–8). Typically, this involved the ankles first, with subsequent progression to the level of the knees and hips. Pyramidal signs (Babinski sign and ankle clonus) were present in the majority of patients, often early into the clinical presentation. Spasticity progressed to involve the upper extremities in a subset of individuals [61%, median age: 21.3 (IQR = 10.6) years versus 32.7 (IQR = 14.6) years in those with no upper extremity involvement]. Lower extremity spasticity was accompanied by weakness in the same distribution. Loss of muscle bulk was present in a subset of patients (10/44), as were contractures of the ankles, knees, or hips (11/37). This was accompanied by significant scoliosis in some (7/34). At last follow-up, approximately 40% of patients were able to walk independently, about 30% patients required a walking aid (cane or walker) and about 30% were dependent on a wheelchair. Pain in the lower extremities, described as 'muscle cramps' or 'muscle spasms' was common and occurred early in the disease course, particularly after long periods of standing, walking, or exercising. In the majority of patients, muscle cramps after exertion or at night were clinically significant, requiring treatment with pain medications, i.e. gabapentin, or muscle relaxants. Extrapyramidal movement disorders were present in the majority of patients (29/44). A postural tremor was present in 8/44 though this was often mild and of limited functional impact. Bradykinesia in combination with rigidity or rest tremor were reported in 7/44, consistent with mild to moderate parkinsonism. There was no significant or sustained benefit from levodopa ($n = 4$). Dystonia, most commonly focal limb or cervical dystonia, was present in about 10%. Ataxia was commonly found, in 28/44, and signs of cerebellar dysfunction included dysarthria ($n = 30$), dysmetria ($n = 9$), intention tremor ($n = 7$), dysdiadochokinesia ($n = 14$) and nystagmus ($n = 12$). Bulbar dysfunction with swallowing dysfunction was reported in four individuals with prolonged disease, but associated comorbidities such as aspiration ($n = 3$) and aspiration pneumonia ($n = 1$) were rare overall.

Urinary symptoms

Symptoms of neurogenic bladder dysfunction were common, often first occurring around the same time as motor symptoms though mild symptoms, such as increased urinary frequency or mild urgency, preceded motor symptoms in some patients. Urinary urgency was prevalent (20/38) whereas more severe symptoms of bladder or bowel dysfunction such as urinary retention (3/40), urinary incontinence (15/41) and bowel incontinence (8/36) were less common.

Sensory symptoms

Sensory symptoms were not systematically assessed in all patients. In the subset of patients with information available, loss of vibration sense and reduced pain sensation in the distal lower extremities were present. Nerve conduction studies were conducted in two individuals and showed axonal sensory neuropathy in one and axonal sensorimotor neuropathy in the other individual.

Cognitive symptoms

Whereas speech delay and learning disabilities were present in early childhood, progressive cognitive impairment occurred after onset of overt motor symptoms. Cognitive dysfunction was rated as mild in 45% (median: 18.3 years, IQR: 5.8), moderate in 24% (median: 21.1 years, IQR: 11.2) and severe in 21% (median: 32.6 years, IQR: 8.1). Formal full-scale IQ testing was available in five individuals showing a range between 40 and 82, though no longitudinal data were available. While it was difficult to quantify cognitive symptoms, loss of previously acquired skills was reported by 29/36 and some adult patients were dependent on help with all activities of daily living.

Other symptoms

Retinopathy was found in four cases, including one case with evidence of retinal macular dystrophy on electroretinogram. No cases of optic nerve atrophy, cataract, ophthalmoplegia, or ptosis were reported. No cases of clinically significant hearing impairment were present. One patient in our cohort experienced seizures. No systemic or other organ-system related symptoms were detected.

Molecular spectrum

Consanguinity was infrequent compared to prior cohorts, occurring in 12/36 families (Table 1). Three-generation family histories were consistent with an autosomal recessive disease but otherwise did not yield any significant patterns. All variants were confirmed to be inherited from an unaffected heterozygous parent. Forty-five distinct variants (14 in a homozygous and 31 in a compound heterozygous state) were identified (Fig. 1A and Supplementary Table 3), including one 459 nucleotide 'out of frame' deletion of exon 22 (c.4373-81_4569 + 181) occurring *in trans* with a multiexon deletion/insertion variant (c.3194_5070delinsAGCTTGCA) affecting exons 18–26 and a previously reported complex chromosomal rearrangement (chr14:67316025_67319414del + g.67316025_67316026insTCTA + g.67319319_67319414inv) resulting in a frameshift [p.(Arg1209fsTer1220)].[6] The latter was identified in a homozygous state in two siblings and a third reportedly unrelated individual from the same geographic region. Recurrent variants in our cohort included the c.5621+1G>T [allele frequency (AF): 8], p.(Ser1312Ter) (AF = 8) and p.(Arg1209fsTer1120) (AF = 6) variants. The majority of identified variants were nonsense ($n = 22$) or frameshift ($n = 12$) variants, predicted to lead to a loss of protein function due to nonsense-mediated mRNA decay. For the single- and multi-exon deletion variants, as well as the additional canonical splice-site variants [c.363+1G>A,

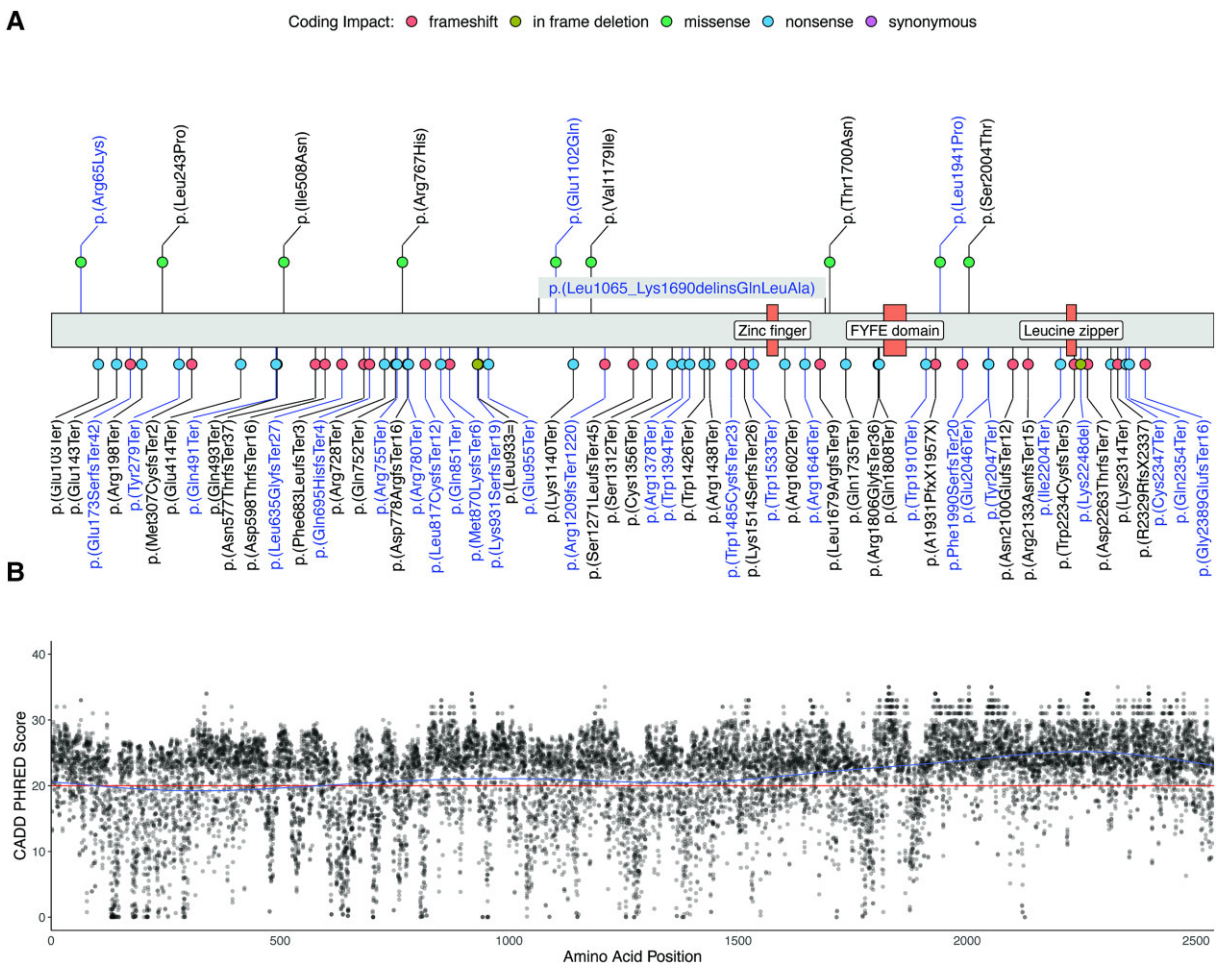

Figure 1 Molecular spectrum of HSP-*ZFYVE26* (SPG15). (**A**) Schematic of the ZFYVE26 primary protein structure. Novel variants identified in our cohort are labelled in blue, previously reported variants are labelled in black. Coding impacts are colour-coded and missense variants are annotated above the protein structure, while all other variants are depicted below. (**B**) CADD PHRED scores for all possible missense variants in *ZFYVE26* were computed and mapped to the linear protein structure. A generalized additive model was used to predict the tolerance for genetic variation across the protein (blue line). The recommended cut-off value for deleteriousness (CADD PHRED = 20) is marked by a red line.

p.(0)?, c.3019+1G>C, p.(0)? and c.7128+1G>C, p.(0)?], the same pathogenic mechanism is postulated. Three unique missense variants were detected in four individuals, one of which carried the homozygous p.(Arg65Lys) variant, while three harboured an additional truncating variant *in trans*. All missense variants were classified as likely pathogenic according to the latest ACMG criteria (Supplementary Table 3). *In silico* analysis revealed CADD PHRED scores above the recommended cut off (CADD PHRED > 20) for all missense variants underscoring their pathogenicity (Supplementary Table 3). Furthermore, two in frame deletion variants [p.(Lys931SerfsTer19) and p.(Lys2248del)], classified as likely pathogenic, and the complex p.(Leu1065_Lys1690delinsGlnLeuAla) delins variant were present in our cohort. Visualization of the spectrum of *ZFYVE26* variants, including previously published disease-causing variants, showed a broad distribution across the primary protein structure without mutational hotspots for missense variants (Fig. 1A). No disease-causing variants mapped to the Zinc finger or FYVE domains, while a single previously reported frameshift variant [p.(Trp2234CysfsTer5)] localized to the leucine zipper domain. Modelling of CADD PHRED scores for all theoretically possible missense variants suggested a high level of intolerability for genomic variation, particularly in the C-terminal region of the ZFYVE26 protein (Fig. 1B).

Neuroimaging findings

Thirty-three patients underwent brain MR imaging (median age at last scan: 19 years, IQR = 10). The most common qualitative findings included: (i) A thin corpus callosum, particularly of the anterior parts (100%; Fig. 2A and B); (ii) T_1-hypointense and T_2-FLAIR hyperintense signal changes in the region of the forceps minor of the corpus callosum consistent with an 'ears of the lynx sign'[16,38] (76%; Fig. 2B and C); (iii) non-specific T_2- or FLAIR-hyperintense signal changes in the periventricular white matter (94%; Fig. 2B and C); (iv) cerebral atrophy (34%; Fig. 2C) and cerebellar atrophy (34%; Fig. 2D). A Venn diagram summarizing these core features is shown in Fig. 2E. An in-depth qualitative and quantitative analysis of 15 brain MRI scans available at Boston Children's Hospital confirmed thinning of the corpus callosum with a thickness of the genu under the 3rd percentile for age in all patients. Diffuse, patchy dysmyelination was seen in the periventricular and periatrial white matter in all cases with 12/15 cases showing a characteristic 'ears of the lynx' configuration. In contrast to other forms of autosomal-recessive HSP with a thin corpus callosum, such as AP-4-associated HSP,[38] the anterior commissure was fully formed in 12/15. The periventricular white matter was mildly to moderately depressed in 8/15

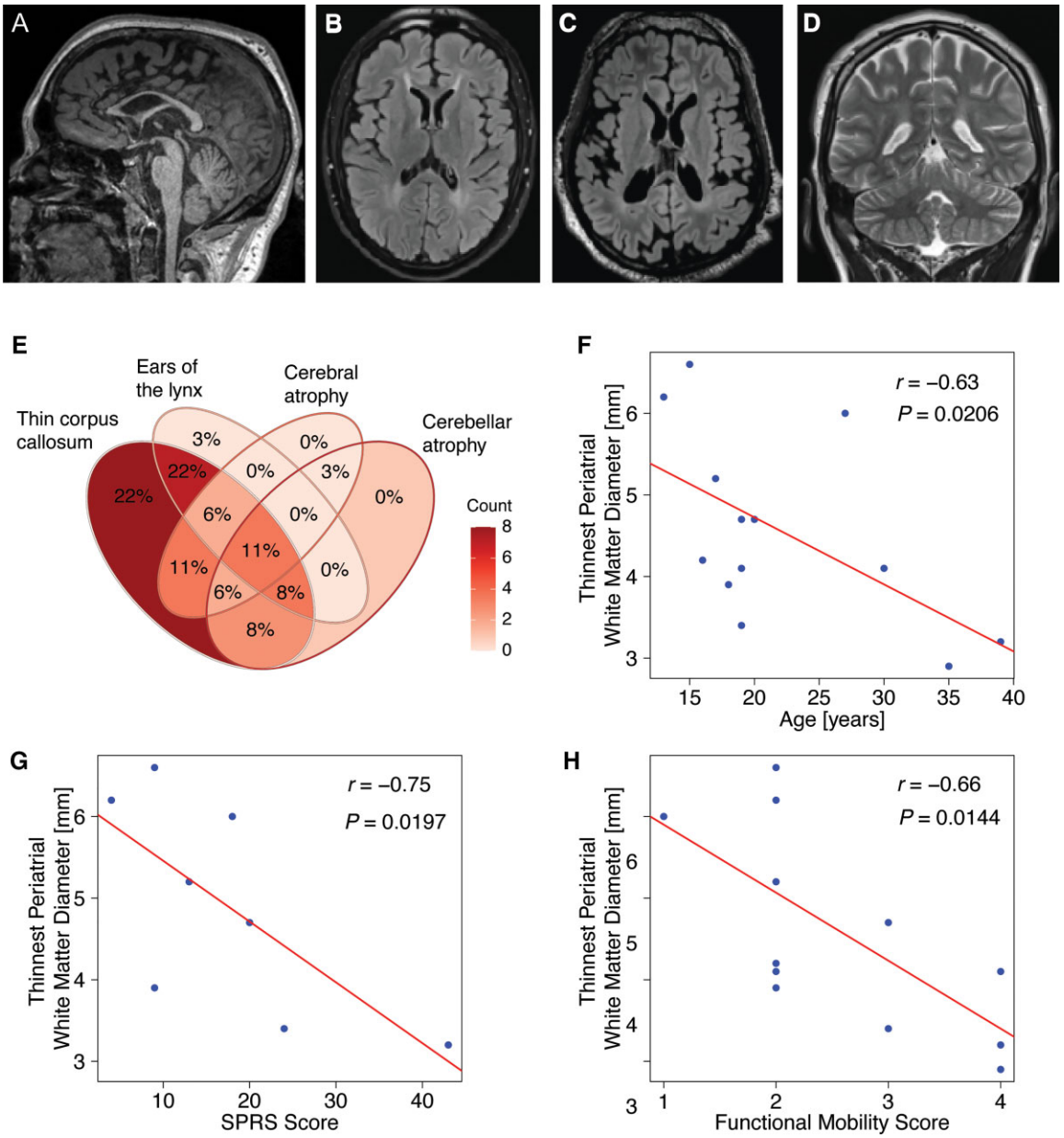

Figure 2 Analysis of the neuroimaging spectrum of HSP-*ZFYVE26* (SPG15) delineates several core features. Key neuroimaging findings in HSP-*ZFYVE26* include thinning of the corpus callosum which predominantly affects the anterior parts (**A**, sagittal T_1-weighted image of an 18-year-old patient). (**B** and **C**) White matter signal changes include a classic 'ears of the lynx' sign as well as diffuse periventricular white matter signal changes (**B**, axial T_2-FLAIR image of an 18-year-old patient). Cerebral volume loss and enlarged lateral ventricles are seen in a subset of patients (**C**, axial T_2-FLAIR image of a 22-year-old patient). (**D**) Cerebellar volume loss is uncommon and usually presents with mild prominence of the cerebellar fissures (coronal T_2-weighted image of an 18-year-old patient). (**E**) Venn diagram of key MRI findings in HSP-*ZFYVE26*. This consists of (i) thinning of the corpus callosum; (ii) abnormal signal of the forceps minor consistent with an 'ears of the lynx' appearance; (iii) cerebral volume loss; and (iv) cerebellar volume loss. (**F–H**) Correlation analysis of MRI findings and clinical characteristics or motor function scores. Red lines represent linear regression lines. Periventricular white matter, approximated using the thinnest periatrial white matter diameter, inversely correlates with age, the SPRS and the Four Stage Functional Mobility Score as an indicator of motor impairment and associated complications.

patients which tended to affect posterior more than anterior regions. Exploratory analysis of correlations between neuroimaging findings and clinical features and motor function scores revealed an inverse correlation of the thinnest periatrial white matter diameter[38] with age, as a surrogate of disease duration (Fig. 2F; $r = -0.63$, $P = 0.0206$), the SPRS (Fig. 2G; $r = -0.75$, $P = 0.0197$) and the Four Stage Functional Mobility Score (Fig. 2H; $r = -0.66$, $P = 0.0144$). Cerebral grey matter volume was reduced in 5/15 patients, while cerebellar atrophy was present in 6/15. No cases of pontine atrophy were found in this sub-cohort of mostly younger patients. Eight patients underwent total spinal cord imaging with no abnormalities identified.

Clinical rating scales and disease progression

The mean SPRS score was 25.2 ± 13.3 (SD), with a mean spasticity subscore (items 7–10) of 7.3 ± 4.3 (SD). Both scores showed moderate strength in representing the proportion of the variation of disease severity from age as a surrogate for disease duration ($R^2_m = 0.51$,

$R^2_c = 0.90$ and $R^2_m = 0.47$, $R^2_c = 0.93$, $P < 0.0001$, respectively), confirming the clinical impression of progressive corticospinal tract dysfunction (Fig. 3A and B). The level of ambulation, as measured on the Four Stage Functional Mobility Score, delineated several clusters, indicating that the SPRS score elevation is largely driven by motor disability (Fig. 3A and B). In the few patients with longitudinal assessments available ($n = 8$ for longitudinal SPRS scores; $n = 28$ for the SPATAX disability score), we found a trajectory of rapid progression. Disease progression over time was also evident in the progression of the SPATAX disability score (mean: 3.2 ± 1.7), $R^2_m = 0.63$, $R^2_c = 0.82$, $P < 0.0001$) (Fig. 3C and D). The distribution of SPATAX disability scores on a cohort level is shown in Fig. 3C. Individual trajectories and inter-individual differences in the rate of progression are highlighted in Fig. 3D. Both the total SPRS and the SPATAX disability score did not show a ceiling effect. In contrast, the predictive value of the Four Stage Functional Mobility Score was limited, likely due to a scale attenuation effect ($R^2_{adj} = 0.25$, $P = 0.0004$; Fig. 3E). A systematic analysis of the age-dependent manifestation and progression of core clinical features is summarized in Fig. 3F. This shows a sequence ranging from developmental symptoms (mainly speech delay, stuttering, and learning disabilities) in early childhood to a first occurrence of motor symptoms in adolescence. The latter consisted of 'clumsiness' early on, followed by gait impairment and lower limb spasticity towards the second decade of life. In this subcohort ($n = 15$), dependency on walking aids or a wheelchair developed soon after onset of lower limb spasticity (at a media age of 17 and 20 years, respectively).

Plasma neurofilament light chain levels

Neurofilament light chain levels are an emerging biomarker in several neurodegenerative diseases,[39] including HSP.[39–41] Plasma NfL levels were measured in 15 patients (median age: 19.5 years, IQR = 10.7) and 15 healthy age controls, mostly matched for age and sex (median age: 20.6 years, IQR = 10.4; Supplementary Table 4). NfL levels were significantly increased in HSP-*ZFYVE26* patients (median: 47.0 pg/ml, IQR = 25.7 versus 3.2 pg/ml, IQR = 1.9 in controls, $P <$ 0.0001, Mann–Whitney U-test; Fig. 4A). Interestingly, while NfL levels remained relatively stable in controls across the age-spectrum covered in this study, NfL level in HSP-*ZFYVE26* patients showed an inverse correlation with age, with larger elevation in younger compared to older patients ($r = -0.65$, $P = 0.01$; Fig. 4B). No correlation with neuroimaging findings or motor scores could be established (not shown).

Treatment

Symptomatic treatment consisted of physical and occupational therapy, baclofen, botulinum toxin injections to treat spasticity and dystonia, and gabapentin for pain associated with muscle cramps.

Levodopa trials were conducted in four individuals but did not lead in any significant improvement of Parkinsonian features.

Core clinical features of HSP-ZFYVE26

A systematic analysis of the HSP-*ZFYVE26* associated disease spectrum, including all previously reported cases ($n = 65$), delineates a set of core clinical features (Box 1 and Fig. 5). A summary of all pertinent clinical features using Human Phenotype Ontology terminology is provided in Supplementary Table 2. Our findings delineate speech delay and learning disability as core clinical features of HSP-*ZFYVE26* (Fig. 5A). While developmental delays were likely underappreciated in prior reports, more than 60% of our patients showed delayed acquisition of speech and/or learning disabilities during childhood. In most cases, developmental delay was mild and did not result in further diagnostic investigations. Gait impairment, as a result of evolving spastic diplegia, ataxia or dystonia, remains the hallmark symptom of HSP-*ZFYVE26*, and a major contributor to morbidity and reduced quality of life. Onset is typically gradual and, in all cases, eventually prompted a referral to a neurologist and genetic testing. Cerebellar dysfunction, mostly consisting of ataxia and dysarthria, was present in more than 60% of our cohort, and seems to have been underappreciated in prior studies (Fig. 5B). Parkinsonism was present in a subset of patients and was associated with significant impact on quality of life. Brain MRI findings were frequently summarized in the literature, in many cases without detailed description or quantitative assessments. Our analysis demonstrates that a characteristic neuroimaging signature, including highly prevalent findings of thinning of the corpus callosum, an 'ears of the lynx' sign and mild to moderate brain atrophy can accelerate the diagnostic process (Fig. 5C).

Discussion

We report cross-sectional data on the clinical and molecular characteristics of 44 patients with molecularly confirmed HSP-*ZFYVE26* (SPG15), the largest cohort assembled to date. For the first time, we provide a detailed assessment of the age-dependent manifestation of clinical symptoms and evaluate several metrics of disease severity and progression.

A review of first clinical symptoms led to the recognition that most patients have a history of speech delay and learning disability; findings that preceded progressive motor symptoms by several years but generally did not lead to a referral to a pediatric neurologist or further diagnostic testing. The reported median age of first developmental concerns was 24 months, while the reported onset of gait or motor impairment was 14.5 years (IQR = 3.5). Initial motor symptoms were often subtle and described as 'clumsiness', 'frequent tripping' or 'stiff legs', particularly during tasks such as running. A concern for HSP was typically raised when progressive gait impairment became apparent, resulting in a molecular diagnosis at a median age of 18.8 years (IQR = 8). Pyramidal signs were often present upon first neurologic evaluation and spasticity would first be noted in the distal legs. In most patients, the spastic diplegia progressed over the course of several years, though anecdotally not in a linear fashion but more commonly in episodic periods of decline. The reported average age of loss of independent ambulation was 17 years (IQR = 5.5). A third of patients ultimately became dependent on a wheelchair, at a mean age of 20 years (IQR = 5).

Beyond pyramidal dysfunction, most patients experienced a slow decline of academic or cognitive abilities, though the rate of this decline was difficult to establish. Most patients had mild intellectual disability at the time of last evaluation. Extra-pyramidal movement disorders in HSP-*ZFYVE26* often included ataxia, usually accompanied by other cerebellar signs such as dysarthria, intention tremor or nystagmus. Dystonia or parkinsonism were less common. Parkinsonism, predominately consisted of bradykinesia, hypomimia, and a rest tremor, and none of the patients treated with levodopa showed any substantial improvement. Signs of a peripheral neuropathy, i.e. loss of deep tendon reflexes in the lower extremities, were present in about 40% of patients, though sensory or autonomic function were not systematically assessed in all patients.

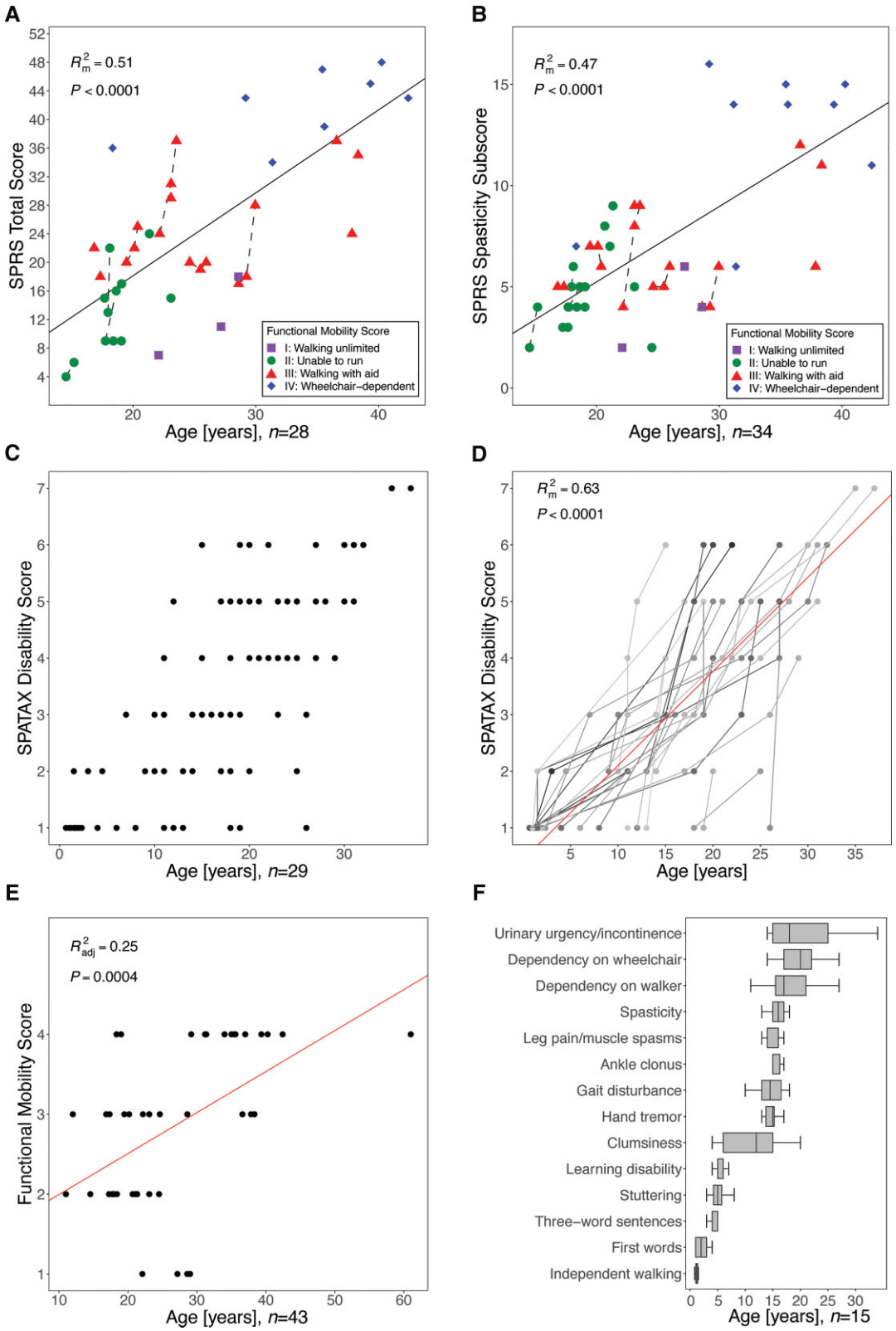

Figure 3 Clinical rating scales reflect disease progression in HSP-*ZFYVE26*. Standardized assessment of disease severity using the (**A**) SPRS score, (**B**) SPRS spasticity subscore, (**C** and **D**) SPATAX disability score (0 = no functional handicap, 1 = no functional handicap but signs on examination, 2 = mild, able to run, walking unlimited, 3 = moderate, unable to run, limited walking without aid, 4 = severe, walking with one stick, 5 = walking with two sticks or four-wheel walker, 6 = unable to walk, requiring wheelchair, 7 = confined to bed) and (**E**) the Four Stage Functional Mobility score (1 = unlimited walking; 2 = walking without aid but unable to run; 3 = walking with aid; and 4 = wheelchair-dependent). The number of individuals included in the respective analyses are indicated below the graphs. Data were modeled using linear regression analysis and, in case of repeated measures collected for some individuals, linear mixed-effects regression analysis. For linear regression models, the adjusted coefficient of determination ($R_{adj}2$) and for linear mixed-effects regression models the marginal coefficient of determination (R^2_m) were reported. *P* values are depicted for each analysis. (**F**) Assessment of age-dependent presentation of clinical signs. Age at first report of the respective symptoms is shown (box plots shows the median and IQR, whiskers indicate minimum and maximum values).

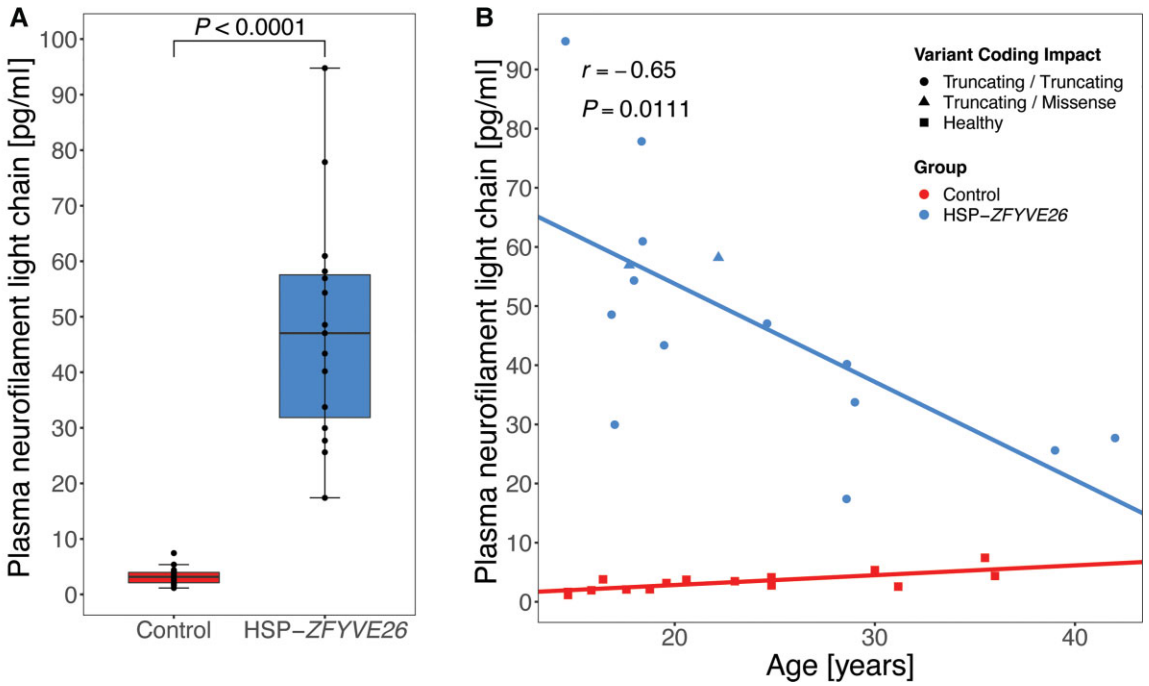

Figure 4 Plasma NfL levels are elevated in HSP-*ZFYVE26*. Plasma NfL levels were measured in 15 HSP-*ZFYVE26* patients and mostly age- and sex-matched controls. (**A**) Absolute NfL levels show a robust separation of patients and controls (Mann–Whitney U-test, $P < 0.0001$). (**B**) Linear model of NfL levels across the age spectrum of the cohort. Variant coding impacts are coded by shape; circles indicate individuals with bi-allelic truncating variants, triangles represent individuals with one truncating variant in *trans* with a missense variant and squares illustrate healthy controls. Correlation analysis was performed using Spearman's rank correlation coefficient.

Box 1 Core clinical and neuroimaging features of HSP-*ZFYVE26* (SPG15)

Core Features (HPO Annotation)	Prevalence
Gait disturbance HP:0001288	92% (84/91)
Spasticity HP:0001257	
• Spastic diplegia HP:0001264	78% (85/109)
• Abnormal pyramidal sign HP:0007256	88% (100/114)
Delayed speech and language development HP:0000750	25% (25/101)
Cognitive impairment HP:0100543	72% (74/103)
Mental deterioration HP:0001268	40% (40/100)
Ataxia HP:0001251	30% (33/109)
Thin corpus callosum HP:0033725	70% (69/98)
'Ears of the lynx' sign	28% (24/86)

The average SPRS score was 25.2, indicating moderate pyramidal dysfunction, with a significant association of higher scores with age, as a surrogate for disease duration. The SPRS spasticity subscore does not depend on ambulation and hence was included in a sub-analysis. This sub-score mirrored the total score with a similar correlation with age. The SPATAX disability score showed a comparable age-dependent evolution but also highlights the inter-individual rates of progression. This loss of motor function over time was also reflected in high rates of patients with need for assisted ambulation or wheelchair-dependence. However, signs of bulbar dysfunction or other complications such as contractures or progressive scoliosis were rare. Neurogenic bladder dysfunction was more common in our cohort compared to published cases, likely reflecting that this symptom is often under-recognized.

Patients with HSP-*ZFYVE26* showed a significant elevation of plasma NfL levels compared to age- and sex-matched controls across the evaluated age-spectrum. NfL levels inversely correlated with age, with the highest levels coinciding around the age at onset of motor disability. We speculate that a rise in plasma NfL could possibly precede overt motor decline. Anecdotally several patients showed a relatively rapid clinical decline in the first 1–2 years following onset of spasticity, with a slower progression thereafter, possibly mirroring the trend seen in NfL levels. No correlations with neuroimaging findings or motor function scores were identified. Despite showing a robust separation of patients and controls, the moderate size of our cohort precludes definitive conclusions about the value of NfL levels as a longitudinal biomarker of disease activity. Larger cohorts and longitudinal measurements of NfL levels will be helpful to evaluate the value as biomarkers for disease severity, individual disease trajectories and the ability to reflect dynamic changes under current or future therapies.

We conclude that core features of HSP-*ZFYVE26*, present in the majority of patients, include spastic diplegia, pyramidal signs, gait impairment, delayed speech development, cognitive decline, and ataxia. While many of these findings are shared with other forms of autosomal-recessive HSP, including HSP-*SPG11*, which is closely linked on a molecular level, there seems to be a relatively uniform timeline of clinical symptoms in HSP-*ZFYVE26*.

Based on this data and our clinical experience, we recommend a multidisciplinary approach to the treatment and surveillance of symptoms in HSP-*ZFYVE26*. Depending on the symptoms present, this may include input from neurology, physiatry, orthopedics, genetics, physical therapy, speech and language pathology, gastroenterology and nutrition, ophthalmology and primary care.[4] Beyond the treatment of spasticity with associated musculoskeletal complications or of extra-pyramidal movement disorders,

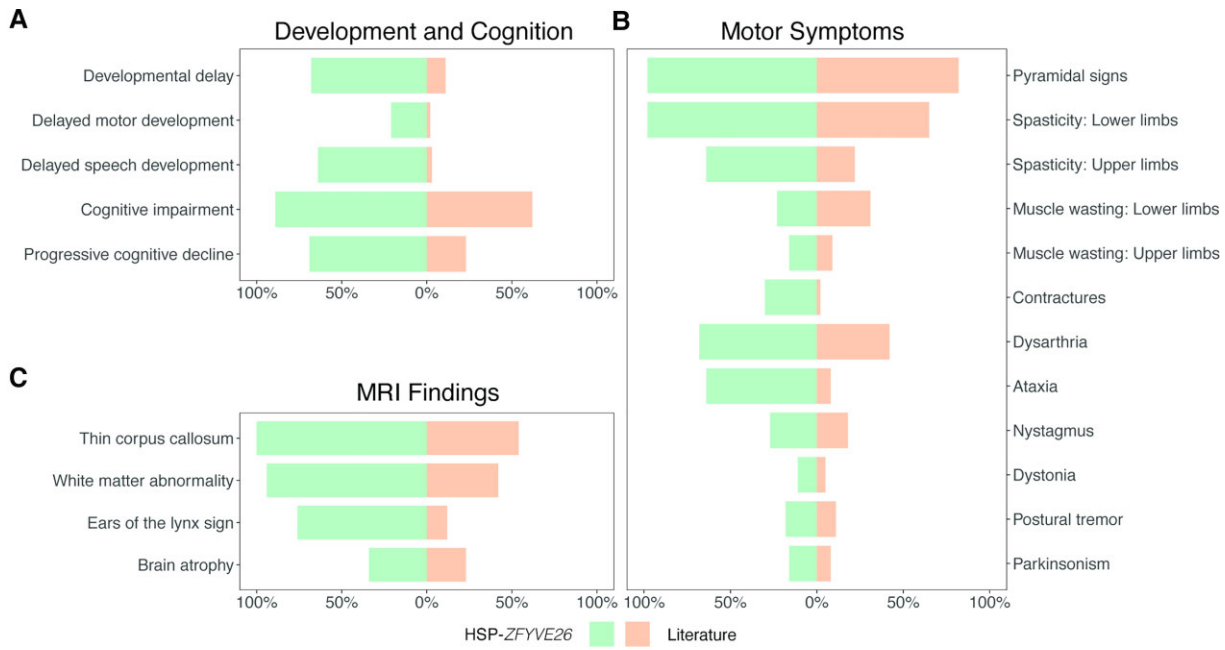

Figure 5 Core clinical features of HSP-*ZFYVE26* in this cohort compared to previously reported cases. Bar plots present the frequency of core clinical features. Individuals with HSP-*ZFYVE26* described in this study ($n = 44$) are depicted in green, while reported cases from the literature are illustrated in orange ($n = 65$).

symptomatic management of speech impairment, neurogenic bladder dysfunction and chronic constipation can improve health-related quality of life. Based on our experience, the prevalence of clinically-relevant retinopathy in HSP-*ZFYVE26* is rare, in contrast to prior reports. Retinopathy-related changes may be detectable on dedicated studies and may present in an age-dependent manner.

The combination of pyramidal dysfunction, extra-pyramidal movement disorders such as ataxia, cognitive decline, retinopathy and peripheral neuropathy in some, suggest a wide-spread neurodegenerative process involving the central and potentially peripheral nervous system. This hypothesis is supported by our review of neuroimaging findings. In addition to the more specific findings of a thin corpus callosum and the signal changes of the anterior forceps of the corpus callosum, we found non-specific atrophy of the cerebral cortex and cerebellum in a subset. While the neuroimaging spectrum of HSP-*ZFYVE26* remains to be defined quantitatively in larger longitudinal cohorts, this supports the wide-spread involvement of different brain areas.

Molecular testing was usually pursued when progressive spasticity or the combination of a thin corpus callosum and spastic diplegia were noted. More patients were diagnosed via exome sequencing than multigene panels, which reflect the shift from panel to broader exome diagnostics as well as its broad use in the research setting. Similar to other genetic diseases, exome sequencing for HSP[42] overcomes several limitations of multigene panels and can reach a diagnostic yield of up to 50%.[43] Analysis of structural variants is important since at least 6% of HSP-associated variants may be small, large or complex structural changes.[43] Disease-causing structural variants in 4/44 cases in our cohort of HSP-*ZFYVE26* confirm their relevance. Most *ZFYVE26* variants identified are single nucleotide variants with predicted truncating effects (stop gained, frameshift or affecting canonical splice site) which supports a loss-of-function mechanism. Contrary to other observations in other HSPs, disease-associated missense variants in *ZFYVE26* do not affect the known functional domains of ZFYVE26 or show any clustering as a hint to a possible molecular mechanism. Identification of crucial interaction sites and functional domains is needed to better understand the molecular impact of missense variants. Thirty percent of families in our cohort harboured homozygous variants, a number driven in part by consanguinity. Compound-heterozygous variants were identified in non-consanguineous families. Recurrent but rare pathogenic alleles within one population or geographic region are suggestive for the theory of 'Clan Genomics'.[44] No clear genotype-phenotype correlations were apparent, likely reflecting the small sample size.

This study has several limitations. Patient recruitment, though representing multiple centres in North America, Europe and East Asia, occurred at tertiary care centres only, possibly introducing a bias towards more severely affected cases. A possible difference to prior published cohorts exists in that most patients in our cohort are located in countries with advanced health care services, whereas prior reports have often focused on cohorts from regions of the world with high rates of consanguinity, which often includes low- and middle-income countries. In our cohort, the age of onset of developmental symptoms was reported by the patients' parents, which may result in inaccurate estimates or recall bias. In addition, since the absence of a given clinical symptom may not be consistently assessed in the literature, our summary of previous reports was based on the total number of reported individuals, irrespective of whether a given symptom was mentioned or not. The prevalence of certain core symptoms might therefore be underestimated. While the cross-sectional data presented here allow for a delineation of core clinical features and an approximation of morbidity across the age spectrum (Fig. 3F), longitudinal natural history studies, beginning in the early oligosymptomatic stages, are needed to define individual disease progression and understand areas of greatest clinical need. The heterogeneity of clinical manifestations,

and likely also of disease progression, discovered in our analysis will inform the choice of outcome parameters for longitudinal studies by helping to prioritize quantitative metrics that are likely to change over the timeframe typical of interventional trials.

Earlier and wide-spread use of next generation sequencing based molecular diagnostics, preferably exome or genome sequencing combined with copy number variant analyses, including for chief complaints such as developmental delay, spasticity or ataxia, will result in an earlier diagnosis of patients with HSP-*ZFYVE26*. Detailed and careful additional phenotyping, following a molecular diagnosis based on a single or set of presenting symptoms, however, will become even more important given the recognition of significant clinical heterogeneity and relevant correlations between genotype and phenotype. Recurrent variants in populations which are underrepresented in public sequencing databases hamper reliable calculation of incidences. As molecular mechanism-based therapies are being developed, an earlier diagnosis and better understanding of the full clinical spectrum of rare forms of HSP will be necessary to design interventional trials.

Acknowledgements

The authors thank the patients and their families for participating in this study. S.E. and H.H. acknowledge support from the Queen Square Genomics consortium. The authors acknowledge material and support from the Precision Link Biobank for Health Discovery at Boston Children's Hospital. The authors acknowledge the SYNaPS Study Group.

Funding

This study was funded by the Deutsche Forschungsgemeinschaft (DFG, German Research Foundation)—(SA 4171/1-1 to A.S.), the International Centre for Genomic Medicine in Neuromuscular Diseases (ICGNMD MR/S005021/1 to S.E.), the Japan Ministry of Health, Labor and Welfare, Grants-in-Aid from the Research Committee for Ataxic Disease (to Y.T.), Italian Ministry of Health (RF-2019-12370112 to A.T. and F.M.S., RC-2021-5X1000 to F.M.S.), CureAP4 Foundation (D.E.F.), the CureSPG50 Foundation (D.E.F.), the Spastic Paraplegia Foundation (D.E.F.), the Manton Center for Orphan Disease Research (D.E.F.), the National Institute of Health/National Institute of Neurological Disorders and Stroke (R25 NS070682 to A.M., 1K08NS123552-01 to D.E.F.), and the Boston Children's Hospital Office of Faculty Development (D.E.F.). The SYNaPS Study Group is funded by The Wellcome Trust (WT093205 MA, WT104033AIA). The Queen Square Genomics group at University College London is supported by the National Institute for Health Research University College London Hospitals Biomedical Research Centre. The BCH Intellectual and the Developmental Disabilities Research Center is supported by the National Institutes of Health (BCH IDDRC, NIH P50 HD105351).

Competing interests

M.S. reports grant support from Novartis, Biogen, Astellas, Aeovian, Bridgebio, and Aucta. He has served on Scientific Advisory Boards for Novartis, Roche, Regenxbio, SpringWorks Therapeutics, Jaguar Therapeutics and Alkermes. D.E.F. received speaker honoraria from the Movement Disorder Society, publishing royalties from Cambridge University Press and reports research funding through a joint research agreement with Astellas Pharmaceuticals Inc. The other authors report no conflict of interest.

Supplementary material

Supplementary material is available at *Brain* online.

Appendix 1

Members of the SYNaPS Study Group who have contributed to this project include: Faisal Zafar, and Nuzhat Rana. Further details are supplied in the Supplementary material.

References

1. Blackstone C. Hereditary spastic paraplegia. *Handb Clin Neurol*. 2018;148:633-652.
2. Ebrahimi-Fakhari D, Saffari A, Pearl PL. Childhood-onset hereditary spastic paraplegia and its treatable mimics. *Mol Genet Metab*. 2022;137(4):436-444.
3. Marras C, Lang A, van de Warrenburg BP, *et al*. Nomenclature of genetic movement disorders: Recommendations of the international Parkinson and movement disorder society task force. *Mov Disord*. 2016;31:436-457.
4. Ebrahimi-Fakhari D, Alecu JE, Blackstone C. Spastic paraplegia 15. In: Adam MP, Ardinger HH, Pagon RA, *et al*. eds. *Genereviews®*. University of Washington; 2021:34057829.
5. Boukhris A, Stevanin G, Feki I, *et al*. Hereditary spastic paraplegia with mental impairment and thin corpus callosum in Tunisia: SPG11, SPG15, and further genetic heterogeneity. *Arch Neurol*. 2008;65:393-402.
6. Hanein S, Martin E, Boukhris A, *et al*. Identification of the SPG15 gene, encoding spastizin, as a frequent cause of complicated autosomal-recessive spastic paraplegia, including Kjellin syndrome. *Am J Hum Genet*. 2008;82:992-1002.
7. Denora PS, Muglia M, Casali C, *et al*. Spastic paraplegia with thinning of the corpus callosum and white matter abnormalities: Further mutations and relative frequency in ZFYVE26/SPG15 in the Italian population. *J Neurol Sci*. 2009;277:22-25.
8. Goizet C, Boukhris A, Maltete D, *et al*. SPG15 Is the second most common cause of hereditary spastic paraplegia with thin corpus callosum. *Neurology*. 2009;73:1111-1119.
9. Schule R, Schlipf N, Synofzik M, *et al*. Frequency and phenotype of SPG11 and SPG15 in complicated hereditary spastic paraplegia. *J Neurol Neurosurg Psychiatry*. 2009;80:1402-1404.
10. Schicks J, Synofzik M, Pétursson H, *et al*. Atypical juvenile parkinsonism in a consanguineous SPG15 family. *Mov Disord*. 2011;26:564-566.
11. Yoon G, Baskin B, Tarnopolsky M, *et al*. Autosomal recessive hereditary spastic paraplegia-clinical and genetic characteristics of a well-defined cohort. *Neurogenetics*. 2013;14:181-188.
12. Mallaret M, Lagha-Boukbiza O, Biskup S, *et al*. SPG15: A cause of juvenile atypical levodopa responsive parkinsonism. *J Neurol*. 2014;261:435-437.
13. Pensato V, Castellotti B, Gellera C, *et al*. Overlapping phenotypes in complex spastic paraplegias SPG11, SPG15, SPG35 and SPG48. *Brain*. 2014;137:1907-1920.
14. Kara E, Tucci A, Manzoni C, *et al*. Genetic and phenotypic characterization of complex hereditary spastic paraplegia. *Brain*. 2016;139:1904-1918.
15. Vinci M, Fchera M, Antonino Musumeci S, Cali F, Aurelio Vitello G. Novel c.C2254T (p.Q752*) mutation in ZFYVE26 (SPG15) gene in a patient with hereditary spastic paraparesis. *J Genet*. 2018;97:1469-1472.
16. Pascual B, de Bot ST, Daniels MR, *et al*. "Ears of the lynx" MRI sign is associated with SPG11 and SPG15 hereditary spastic paraplegia. *AJNR Am J Neuroradiol*. 2019;40:199-203.

17. Özdemir TR, Gençpınar P, Arican P, Öztekin O, Dündar NO, Özyılmaz B. A case of spastic paraplegia-15 with a novel pathogenic variant in *ZFYVE26* gene. *Int J Neurosci*. 2019;129:1198-1202.
18. Araujo FMM, Junior WM, Tomaselli PJ, Pimentel AV, Macruz Brito MC, Tumas V. SPG15: A rare correlation with atypical juvenile parkinsonism responsive to levodopa. *Mov Disord Clin Pract*. 2020;7:842-844.
19. Renvoise B, Chang J, Singh R, *et al*. Lysosomal abnormalities in hereditary spastic paraplegia types SPG15 and SPG11. *Ann Clin Transl Neurol*. 2014;1:379-389.
20. Koh K, Ishiura H, Tsuji S, Takiyama Y. JASPAC: Japan spastic paraplegia research consortium. *Brain Sci*. 2018;8:153.
21. Richards S, Aziz N, Bale S, *et al*. Standards and guidelines for the interpretation of sequence variants: A joint consensus recommendation of the American college of medical genetics and genomics and the association for molecular pathology. *Genet Med*. 2015;17:405-424.
22. Ebrahimi-Fakhari D, Teinert J, Behne R, *et al*. Defining the clinical, molecular and imaging spectrum of adaptor protein complex 4-associated hereditary spastic paraplegia. *Brain*. 2020;143:2929-2944.
23. Schule R, Holland-Letz T, Klimpe S, *et al*. The Spastic Paraplegia Rating Scale (SPRS): A reliable and valid measure of disease severity. *Neurology*. 2006;67:430-434.
24. Chrestian N, Dupre N, Gan-Or Z, *et al*. Clinical and genetic study of hereditary spastic paraplegia in Canada. *Neurol Genet*. 2017;3:e122.
25. Kohler S, Gargano M, Matentzoglu N, *et al*. The human phenotype ontology in 2021. *Nucleic Acids Res*. 2021;49:D1207-D1217.
26. Wildeman M, van Ophuizen E, den Dunnen JT, Taschner PE. Improving sequence variant descriptions in mutation databases and literature using the Mutalyzer sequence variation nomenclature checker. *Hum Mutat*. 2008;29:6-13.
27. Kopanos C, Tsiolkas V, Kouris A, *et al*. Varsome: The human genomic variant search engine. *Bioinformatics*. 2019;35:1978-1980.
28. Li Q, Wang K. Intervar: Clinical interpretation of genetic variants by the 2015 ACMG-AMP guidelines. *Am J Hum Genet*. 2017;100:267-280.
29. UniProt C. Uniprot: The universal protein knowledgebase in 2021. *Nucleic Acids Res*. 2021;49:D480-D489.
30. Hsu SL, Lu YJ, Tsai YS, *et al*. Investigating ZFYVE26 mutations in a Taiwanese cohort with hereditary spastic paraplegia. *J Formos Med Assoc*. 2022;121:126-133.
31. Rentzsch P, Witten D, Cooper GM, Shendure J, Kircher M. CADD: Predicting the deleteriousness of variants throughout the human genome. *Nucleic Acids Res*. 2019;47:D886-D894.
32. Stephenson JD, Laskowski RA, Nightingale A, Hurles ME, Thornton JM. Varmap: A web tool for mapping genomic coordinates to protein sequence and structure and retrieving protein structural annotations. *Bioinformatics*. 2019;35:4854-4856.
33. Neuser S, Brechmann B, Heimer G, *et al*. Clinical, neuroimaging, and molecular spectrum of TECPR2-associated hereditary sensory and autonomic neuropathy with intellectual disability. *Hum Mutat*. 2021;42:762-776.
34. Altmann P, Ponleitner M, Rommer PS, *et al*. Seven day preanalytical stability of serum and plasma neurofilament light chain. *Sci Rep*. 2021;11:11034.
35. Nakagawa S, Schielzeth H. A general and simple method for obtaining R^2 from generalized linear mixed-effects models. *Methods Ecol Evol*. 2013;4:133-142.
36. Sotirchos ES, Fitzgerald KC, Crainiceanu CM. Reporting of R^2 statistics for mixed-effects regression models. *JAMA Neurol*. 2019;76:507.
37. Bibi F, Efthymiou S, Bourinaris T, *et al*. Rare novel CYP2U1 and ZFYVE26 variants identified in two Pakistani families with spastic paraplegia. *J Neurol Sci*. 2020;411:116669.
38. Ebrahimi-Fakhari D, Alecu JE, Ziegler M, *et al*. Systematic analysis of brain MRI findings in adaptor protein Complex 4-associated hereditary spastic paraplegia. *Neurology*. 2021;97:e1942-e1954.
39. Gaetani L, Blennow K, Calabresi P, Di Filippo M, Parnetti L, Zetterberg H. Neurofilament light chain as a biomarker in neurological disorders. *J Neurol Neurosurg Psychiatry*. 2019;90:870-881.
40. Wilke C, Rattay TW, Hengel H, *et al*. Serum neurofilament light chain is increased in hereditary spastic paraplegias. *Ann Clin Transl Neurol*. 2018;5:876-882.
41. Kessler C, Serna-Higuita LM, Rattay TW, *et al*. Neurofilament light chain is a cerebrospinal fluid biomarker in hereditary spastic paraplegia. *Ann Clin Transl Neurol*. 2021;8:1122-1131.
42. Saputra L, Kumar KR. Challenges and controversies in the genetic diagnosis of hereditary spastic paraplegia. *Curr Neurol Neurosci Rep*. 2021;21:15.
43. Méreaux JL, Banneau G, Papin M, *et al*. Clinical and genetic spectra of 1550 index patients with hereditary spastic paraplegia. *Brain*. 2022;145:1029-1037.
44. Lupski JR, Belmont JW, Boerwinkle E, Gibbs RA. Clan genomics and the complex architecture of human disease. *Cell*. 2011;147:32-43.